Spin Drift Velocity, Polarization, and Current-Driven Domain-Wall Motion in (Ga,Mn)(As,P)

J. Curiale,[1,2,*] A. Lemaître,[2] C. Ulysse,[2] G. Faini,[2] and V. Jeudy[1,3,†]

[1]*Laboratoire de Physique des Solides, Université Paris-Sud, CNRS, 91405 Orsay, France*
[2]*Laboratoire de Photonique et de Nanostructures, CNRS, 91460 Marcoussis, France*
[3]*Université Cergy-Pontoise, 95000 Cergy-Pontoise, France*

Current-driven domain-wall motion is studied in (Ga,Mn)(As,P) ferromagnetic semiconducting tracks with perpendicular anisotropy. A linear steady state flow regime is observed over a large temperature range of the ferromagnetic phase ($0.1T_c < T < T_c$). Close to 0 K, the domain-wall velocity is found to coincide with the spin drift velocity. This result is obtained below the intrinsic threshold for domain-wall motion which implies a nonadiabatic contribution to the spin transfer torque. The current spin polarization is deduced close to 0 K and to T_c. It suggests that the temperature dependence of the spin polarization can be inferred from the domain-wall dynamics.

A spin polarized current flowing through a domain wall (DW) exerts a torque on the DW magnetization. At sufficiently large current, this torque produces DW motion. In the damping limited flow regimes, the DW dynamics is commonly derived from a modified Laudau-Lifshitz-Gilbert equation [1,2]. Within this phenomenological description, two contributions to the spin torque are usually introduced: an *adiabatic* term, and a *nonadiabatic* contribution, proportional to the so-called β factor. The predicted DW velocities v are proportional to the spin drift velocity of the current carriers and depend on the ratio β/α, where α is the Gilbert damping coefficient. Several authors have carried out microscopic derivations of β and α from spin relaxation mechanisms due to impurity scattering in metals [3], or due to spin-orbit interaction [4,5]. However, these predictions are rather different and can hardly be compared quantitatively to the limited number of experimental results.

Experimentally, the damping limited flow regimes are difficult to reach due to the high current density threshold Jth required to move DWs. For metallic structures, linear flow regimes $v(J)$ were observed only recently, in Pt/Co/AlO$_x$ tracks [6] with perpendicular anisotropy ($J_{\text{th}} = 10^{12}$ A/m^2). In (Ga,Mn)As ferromagnetic semiconductors, flow regimes were evidenced ($J_{\text{th}} = 10^9$ A/m^2 [7]) only close to the Curie temperature in layers with perpendicular magnetic anisotropy [7,8]. A β/α value close to 1 was deduced from the analysis of current-induced domain-wall dynamics [7], performed in the frame of the 1D model [1,2]. However, this result remains puzzling since the α values deduced from field-driven measurements [7,9] strongly differ from theoretical predictions and ferromagnetic resonance measurements. Obviously a better understanding of the fundamental physics of current-driven DW dynamics would benefit from a model-independent determination of the parameters governing DW motion, such as the carrier spin polarization and the

spin drift velocity. Moreover, it would be particularly interesting to study DW motion at low temperature. Indeed, to our best knowledge, carrier spin polarization in (Ga,Mn)As was only estimated close to zero temperature [10–12], from point-contact Andreev reflection measurements. Reducing the temperature would also decrease the thermal fluctuations which may significantly affect DW dynamics [13].

In previous studies, the flow regime was only accessible in a narrow temperature range below T_c. These experiments were performed on (Ga,Mn)As tracks grown on metamorphic (In,Ga)As substrates [7,8], required to provide a perpendicular anisotropy. However, the metamorphic growth mode is inherently associated with the formation of emerging dislocations [14] and other defects which act as pinning centers for DWs. Moreover, the low heat conductivity of (In,Ga)As substrates [15,16] results in a large track temperature rise produced by Joule heating which impedes the exploration at low temperature. Recently, we developed a new alloy (Ga,Mn)(As,P) grown pseudomorphically on GaAs substrate [17], presenting a perpendicular anisotropy. Current-driven DW motion has been reported in this alloy well below T_c [18].

In this Letter, we present a thorough investigation of the linear flow regime in (Ga,Mn)(As,P) tracks over the whole temperature range, from $\sim 0.1T_c$ ($T = 13$ K) up to T_c. DW velocity v is shown, without any assumptions on the nature of the flow regime, to coincide with the carrier spin drift velocity u, close to 0 K. Rather interestingly, these experiments suggest that DW dynamics give access to the current spin polarization P_c over the whole temperature range up to T_c.

The micro-tracks with a perpendicular magnetic anisotropy were elaborated [17] from a 50 nm thick $(Ga_{0.90}Mn_{0.10})(As_{0.89}P_{0.11})$ film, deposited by molecular beam epitaxy on a 375 μm thick GaAs (001) substrate at $T = 250\,°C$. The film was then annealed during 1 h, at

$T = 250\,°C$. The Curie temperature of the film is $T_c = 119 \pm 1$ K. For the details on experimental methods, see Supplemental Material [19]. Micro-tracks 90 μm long, oriented along the $[1\bar{1}0]$, $[110]$, and $[100]$ axes with different widths (0.5, 1, 2, 4 μm), and connected to a nucleation pad, were patterned by e-beam lithography. The saturation magnetization $M_s(T)$ was determined from magnetometry measurements (SQUID). The estimated effective Mn spin concentration is 5% [19]. Current-induced DW motion was studied in an open cycle optical cryostat with a temperature accuracy of 0.2 K. DW motion is produced by current pulses of different amplitudes J and of a *single* duration $\Delta t = 1\ \mu$s. The magnetic state of the tracks was observed by differential polar magneto-optical Kerr microscopy with a 1 μm resolution. As the DW displacements Δx were found to be proportional to the pulse duration and to the number of pulses, the average DW velocity is defined as $v = \Delta x / \Delta t$ [7,19]. The Joule heating of the track due to current pulses was studied extensively [15] and carefully taken into account (see [19]). In order to compare DW dynamics for a fixed track temperature T, for each J value, the sample holder was set to an initial temperature $T_i = T - \Delta T(J, 1\ \mu$s$)$, where $\Delta T(J, 1\ \mu$s$)$ is the temperature rise at the end of the pulse. For the lowest explored temperature $T = 13$ K, the initial temperature was set to $T_i = 4$ K for $J = 13$ GA/m^2.

The current-driven DW velocity v is reported in Fig. 1 as a function of the current density for several temperatures. DW motion is observed over a large temperature range (13 K $< T <$ 110 K). Three different regimes can be identified [7,8]. At low values of the current density J (see inset of Fig. 1, $T = 95$ K), DWs move in a creep regime dominated by pinning barriers and thermal activation. Their

velocity is low ($v < 0.1$ m/s) and varies exponentially with J. For $J > J_{\text{dep}} \approx 5$ GA/m^2 ($T = 95$ K), v becomes larger than ~ 1 m/s. DWs move in a depinning regime controlled by pinning and dissipation. For $J > J_{\text{fl}} \approx 11$ GA/m^2 ($T = 95$ K), DW motion enters a linear flow regime, only limited by dissipation. This linear regime, whose nature is discussed later, is observed for each temperature. The linear extrapolation to zero current yields $v = 0$ m/s, within the experimental errors (see [19]). In this flow regime, the current DW mobility, defined as $\mu_J = v/J$, decreases as the temperature is lowered from 105 to 42.5 K. At lower temperature, μ_J becomes weakly temperature dependent, as evidenced by two additional velocity values measured at 28 and 13 K, which fall close to the curve obtained at 42.5 K. A characteristic slope change indicates the transition from the depinning regime to the linear one, which gives a determination of the linear regime lower bound: $J_{\text{fl}}(T) = 5.5,\ 11,\ 13$ GA/m^2 for $T = 105,\ 95,$ and 42.5 K, respectively.

To get a better insight into the temperature variations of the DW mobility $\mu_J = v/J$, DW dynamics was studied as a function of the temperature for three different current densities. Results are reported in Fig. 2. For the lowest density $J = 7.0 \pm 0.5$ GA/m^2 (circles), μ_J decreases strongly as T is reduced. The DW dynamics crosses the boundary between the flow and the depinning regimes and eventually the DWs become pinned ($\mu_J = 0$) at finite temperature ($T \approx 70$ K). For the intermediate density $J = 11.5 \pm 1.8$ GA/m^2 (triangles), a pronounced temperature variation is also observed for $T > 80$ K. Below 80 K, μ_J is almost independent of temperature (≈ 0.5 mm^3/C). As $J < J_{\text{fl}}(T)$, the flow regime threshold, this could be the
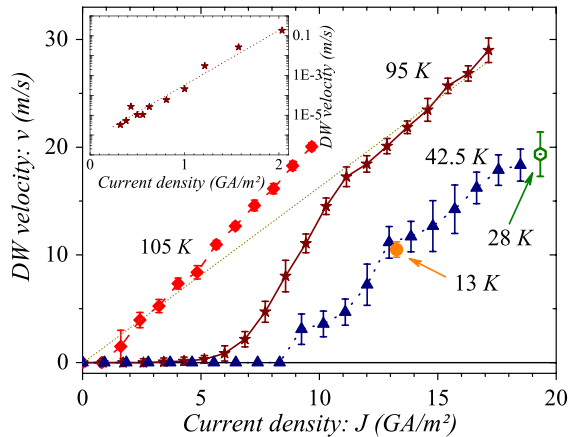

FIG. 1 (color online). Current-driven DW velocity v measured at different temperatures T. Each point and its error bar correspond to the average and to the standard deviation calculated with more than 20 measurements, respectively. At $T = 42.5$ K, larger error bars also reflect a slight asymmetry of DW displacements found as the current is reversed. Inset: Semilogarithmic plot of v measured at 95 K for the lowest current densities.
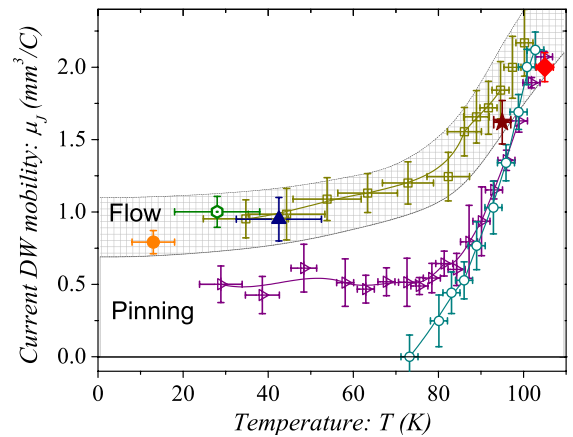

FIG. 2 (color online). Temperature variations of the current mobility ($\mu_J = v/J$). The empty symbols correspond to three different current values: 13.3 ± 2.0 GA/m^2 (squares), 11.5 ± 1.8 GA/m^2 (triangles), and 7.0 ± 0.5 GA/m^2 (circles). The filled symbols correspond to the boundary between the pinning controlled and the flow linear regimes, deduced form the slope changes observed in Fig. 1. The flow linear regime is materialized by a shaded area.

signature of a DW motion controlled by a distribution of energy barriers [20]. For the highest current density $J = 13.3 \pm 2.0$ GA/m^2 (squares) the curve goes through the μ_J values already reported in Fig. 1 for the linear regime ($J \geq J_{fl}$). The current-induced linear flow regime is thus evidenced over the whole temperature range (13 K < T < 110 K).

We now focus on the origin of the temperature variations of μ_J for the flow regime. As the DW velocity v is proportional to the current density J, we write $v = r_{fl}(T)u$, where $r_{fl}(T)$ is to be determined. The spin drift velocity is $u = \frac{JP_c(T)g\mu_B}{2eM_s(T)}$ [1,2], where g, μ_B, e, and $P_c(T)$ are the Landé factor, the Bohr magneton, the electron charge, and the current spin polarization, respectively. Close to 0 K, u can be deduced from $M_s(T \sim 0$ K) (Fig. 3) and $P_c(T \sim 0$ K). P_c was estimated close to 4 K from point-contact Andreev reflection spectroscopy for (Ga,Mn)As samples with similar Mn concentrations: $P_c \approx 0.75$, 6% Mn [10]; $P_c > 0.85$, 5% Mn [11], and $P_c = 0.57$, 7% Mn [12]. Taking the values from Refs. [10,12] we get $u = 8.5$–11.2 m/s for $J = 13.3$ GA/m^2. We now compare these values to the DW velocity v with the same current density, at 13 K. $v = 10.5 \pm 0.7$ m/s, a value very close to the spin drift velocity u at 4 K, i. e., $r_{fl} \sim 1$ for $T \sim 0$ K. In order to determine to what extent this result is valid for other temperatures, the current spin polarization $P_c^{DW}(T)$ deduced from DW dynamics is plotted in Fig. 3, assuming $r_{fl}(T) = 1$. Values of $P_c^{DW}(T)$ are calculated using the measured magnetization $M_s(T)$ (see Fig. 3) and current mobility $\mu_J(T)$, for $J \geq J_{fl}$ (see Fig. 2). Results obtained close to T_c with an annealed (Ga$_{0.93}$, Mn$_{0.07}$)As 4 μm wide track, with similar Mn concentration [21] are also reported in Fig. 3. The temperature variations for both (Ga,Mn)As and (Ga,Mn)(As,P) tracks shows similar trends close to T_c.
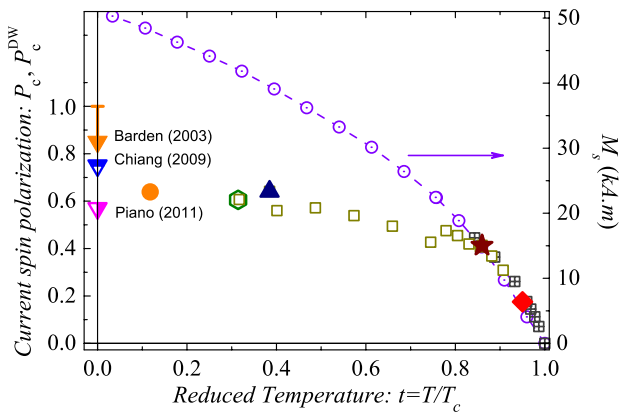

FIG. 3 (color online).   Temperature variation of the spin polarization P_c^{DW} deduced from domain-wall dynamics (left scale: same legend as for Fig. 2) and of the magnetization M_s (right scale: ⊙). Values of the spin polarization P_c (left scale: down triangles) deduced from point-contact Andreev reflection measurements [10–12]. The crossed symbols (⊞) correspond to results obtained for P_c^{DW}, with (Ga$_{0.93}$, Mn$_{0.07}$)As μm wide tracks.

The curve extrapolates to $P_c^{DW} = 0.67 \pm 0.03$, for $T \to 0$ K. As shown in Fig. 3, this value is found in between the estimations of P_c given in Refs. [10,12]. Taking those estimations as boundaries for P_c^{DW}, it follows that $0.85 < r = v/u < 1.12$, close to 0 K. This is a key result of this Letter. It shows that a rather accurate estimation of the current spin polarization can be deduced from current-induced DW dynamics. Moreover, it demonstrates, without adjustable parameter, that the domain-wall velocity v is quantitatively close to the spin drift velocity u, for $T \approx 0$ K.

The generalization of this result far from 0 K is not straightforward due to the lack of estimations of P_c values. However, the following shows that $u \approx v$ is compatible with experimental results, close to the Curie temperature. As observed in Fig. 3, $P_c^{DW} \to 0$ for $t = T/T_c \to 1$. Indeed the spin polarization tends to zero with the collapse of hole mediated ferromagnetism. Moreover, $P_c^{DW}(T)$ follows the temperature variation of $M_s(T)$. This observation is consistent with the predictions of Dietl *et al.* [8,22], close to T_c, where the thermodynamic spin polarization $P(T) = \frac{6k_BT_C}{(S+1)pJ_{pd}}\frac{M_s(T)}{M_s(T=0)}$. k_B, J_{pd}, S, and p are the Boltzmann constant, the exchange integral ($J_{pd} = -54$ meV nm^3), the Mn spin ($S = 5/2$), and the carrier density, respectively. If we assume $P_c^{DW}(T) = 1.0$–$1.8P(T)$, (the upper boundary is proposed in Ref. [12], close to 0 K), the carrier density p can be deduced from $P_c^{DW}(T)$ and $M_s(T)$ (Fig. 3) and the predictions for $P(T)$. The obtained values are $p \approx 0.18$–0.32 nm^{-3} and $p \approx 0.23$–0.42 nm^{-3} for the (Ga,Mn)(As,P) and (Ga,Mn)As tracks, respectively. The carrier densities for both materials are rather close and compatible with the somewhat larger resistivity measured for (Ga,Mn)(As,P) (a factor two) [14,23]. The same orders of magnitude were deduced from other experimental methods in samples exhibiting similar magnetic properties, as reported in Ref. [21]. Therefore, the measured temperature variations of μ_J are also compatible with $v \approx u$, close to T_c. An alternative analysis based on the Döring inequality leads to the same conclusion, as reported in Refs. [7,21].

The fact that $v \approx u$ close to 0 K and to T_c, strongly suggests that for the linear flow regime, the temperature variation of the current mobility μ_J is essentially determined by the ratio $P_c(T)/M_s(T)$ between the current spin polarization and the magnetization. In this respect, the curve $P_c^{DW}(T)$ (obtained for $v = u$) reported in Fig. 3 does reflect the temperature variation of the current spin polarization.

We now discuss the nature of the linear flow regime and the nonadiabaticity of the spin transfer torque. In Fig. 4, the reduced DW velocity v/v_w predicted by the 1D model [1,2] is plotted as a function of the reduced spin drift velocity u/v_w, where v_w is the so-called Walker velocity, for different values of β/α. Two linear flow regimes are predicted to occur (see the curves obtained for $\beta/\alpha = 8$ and 1/8). For the lowest u values, DWs move in the steady
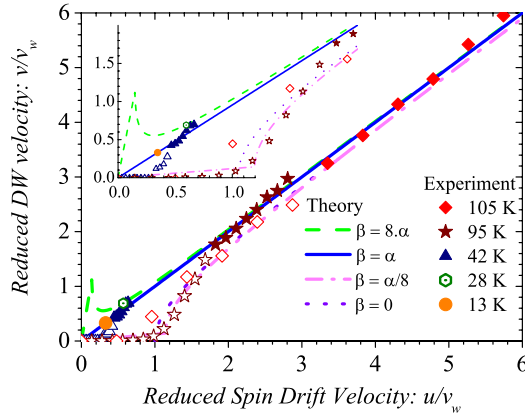
FIG. 4 (color online). Comparison between the experimental results and predictions for the domain-wall flow regimes. Filled (empty) symbols correspond to the flow (depinning) regime. Inset. Zoom for low values of the reduced spin drift velocity u/v_w.

state flow regime whenever the magnetization direction within the DW remains constant with time. In this regime, the velocity $v = (\beta/\alpha)u$. Above the so-called Walker limit, the motion becomes nonlinear with current: DWs are in the precessional regime (the direction of the DW magnetization precesses during the DW motion). For higher u values, DWs follow the asymptotic precessional regime for which $v = u$. Let us note that no steady state regime is predicted for $\beta/\alpha = 0$, while no precessional regime should occur for $\beta/\alpha = 1$. In that specific case, the DW motion would remain in the steady state regime for any arbitrary large current.

Figure 4 also reports experimental results deduced from Fig. 1. The Walker velocities are obtained from $v_w = \mu_0 \gamma M_s(T)\Delta/2$, where the wall thickness parameter $\Delta = 6.5 \pm 1.0$ nm is taken from Ref. [24]. u is estimated from the values of $P_c^{DW}(T)$ and of $M_s(T)$ reported in Fig. 3. It is worth noting that the u/v_w values span over more than 1 order of magnitude ($0.3 < u/v_w < 6$) because of the large $M_s(T)$ change over the investigated temperature range. In the linear flow regime, the reduced domain-wall velocities (filled symbols) gather onto a single linear master curve since we assumed that $v = u$. The points departing from the $v = u$ line (empty symbols) correspond to DW motion occurring in the depinning regime, as discussed previously. The coincidence between the points measured $T = 95$ and 105 K in the depinning regime (empty symbols) and the flow regime predictions for $\beta/\alpha = 0$ and 1/8 is therefore accidental.

As seen in Fig. 4, DW motion occurs in the flow regime well below the intrinsic DW motion threshold $u/v_w = 1$ expected for a purely adiabatic spin transfer torque. This is a clear evidence of a nonadiabatic contribution (i.e., $\beta \neq 0$) to the spin transfer torque, in contradiction with the conclusions of Ref. [8]. Two different ranges of β/α values would reproduce our experimental data. A good agreement

is obtained with the predicted steady regime, for $\beta/\alpha = 1$. The experimental results seem to be also compatible with the asymptotic precessional regime for $\beta/\alpha = 8$, as predicted in Ref. [4]. A higher β/α ratio, as proposed in Ref. [5], would shift the Walker peak towards lower values of u/v_w and improve the quantitative agreement. In order to discriminate between the steady state and the precessional regimes, experiments combining current and magnetic field-induced motion of magnetic *domains* were performed, as proposed in Ref. [7]. Weak magnetic fields are applied ($-5 < H < 5$ Oe) during the current pulse. The magnetic field DW mobility $\mu_H = dv/\mu_0 dH$ is then extracted and compared to mobilities measured in experiments where both flow regimes have been clearly identified [9]. Close to $T = 0$ K, the measured magnetic field mobility $\mu_H = 2.3 \pm 0.4$ m/s mT. This value is close to the DW mobility in the steady state regime ($\mu_H = 1.6 \pm 0.5$ m/s mT) deduced from field-induced DW motion in (Ga,Mn)As films [9] with similar Mn concentration. It is far larger than the mobility ($\mu_H = 0.11 \pm 0.02$ m/s mT) measured in the asymptotic precessional regime. Therefore this experiment clearly supports the hypothesis of DW motion in the steady state regime (i.e., $\beta \neq 0$) and, in the frame of the 1-D model, a ratio β/α close to 1.

Our investigations on current-induced domain-wall motion have evidenced a linear domain-wall flow regime over a wide range of temperatures ($0.1T_c < T < T_c$). Domain walls were shown to move in the steady state regime with velocities corresponding to the carrier spin drift velocities. Hence, we inferred that the β term, characterizing the nonadiabatic spin transfer torque, is close to the Gilbert damping coefficient. Moreover, our results suggest that DW dynamics give direct access to the temperature variation of the current spin polarization. This parameter is crucial for understanding the spin transfer phenomena. However its estimation is not straightforward experimentally [25,26].

---

*Now at Consejo Nacional de Investigaciones Científicas y Técnicas, Centro Atómico Bariloche Comisión Nacional de Energía Atómica, Avenida Bustillo 9500, 8400 S. C. de Bariloche, Río Negro, Argentina
†vincent.jeudy@u-psud.fr

[1] S. Zhang and Z. Li, Phys. Rev. Lett. **93**, 127204 (2004).
[2] A. Thiaville, Y. Nakatani, J. Miltat, and Y. Suzuki, Europhys. Lett. **69**, 990 (2005).

[3] G. Tatara, H. Kohno, and J. Shibata, Phys. Rep. **468**, 213 (2008).

[4] I. Garate, K. Gilmore, M. D. Stiles, and A. H. MacDonald, Phys. Rev. B **79**, 104416 (2009).

[5] K. M. D. Hals, A. K. Nguyen, and A. Brataas, Phys. Rev. Lett. **102**, 256601 (2009).

[6] I. M. Miron *et al.*, Nature Mater. **10**, 419 (2011).

[7] J.-P. Adam, N. Vernier, J. Ferré, A. Thiaville, V. Jeudy, A. Lemaître, L. Thevenard, and G. Faini, Phys. Rev. B **80**, 193204 (2009).

[8] M. Yamanouchi, D. Chiba, F. Matsukura, T. Dietl, and H. Ohno, Phys. Rev. Lett. **96**, 096601 (2006).

[9] A. Dourlat, V. Jeudy, A. Lemaître, and C. Gourdon, Phys. Rev. B **78**, 161303(R) (2008).

[10] T. W. Chiang, Y. H. Chiu, S. Y. Huang, S. F. Lee, J. J. Liang, H. Jaffré, J.-M. George, and A. Lemaître, J. Appl. Phys. **105**, 07C507 (2009).

[11] J. G. Braden, J. S. Parker, P. Xiong, S. H. Chun, and N. Samarth, Phys. Rev. Lett. **91**, 056602 (2003).

[12] S. Piano, R. Grein, C. J. Mellor, K. Vyborny, R. Campion, M. Wang, M. Eschrig, and B. L. Gallagher, Phys. Rev. B **83**, 081305(R) (2011).

[13] M. E. Lucassen, H. J. van Driel, C. Morais Smith, and R. A. Duine, Phys. Rev. B **79**, 224411 (2009).

[14] L. Thevenard, L. Largeau, O. Mauguin, G. Patriarche, A. Lemaître, N. Vernier, and J. Ferré, Phys. Rev. B **73**, 195331 (2006).

[15] J. Curiale, A. Lemaître, G. Faini, and V. Jeudy, Appl. Phys. Lett. **97**, 243505 (2010).

[16] S. Adachi, J. Appl. Phys. **54**, 1844 (1983).

[17] A. Lemaître, A. Miard, L. Travers, O. Maugin, L. Largeau, C. Gourdon, V. Jeudy, M. Tran, and J.-M. Georges, Appl. Phys. Lett. **93**, 021123 (2008).

[18] K. Y. Wang, K. W. Edmonds, A. C. Irvine, G. Tatara, E. de Ranieri, J. Wunderlich, K. Olejnik, A. W. Rushforth, R. P. Campion, D. A. Williams, C. T. Foxon, and B. L. Gallagher, Appl. Phys. Lett. **97**, 262102 (2010).

[19] See Supplemental Material at http://link.aps.org/supplemental/10.1103/PhysRevLett.108.076604 for detailed samples information, the determination of domain-wall velocity, and the correction of Joule heating..

[20] B. Barbara and W. Wernsdorfer, Curr. Opin. Solid State Mater. Sci. **2**, 220 (1997).

[21] V. Jeudy, J. Curiale, J.-P. Adam, A. Thiaville, A. Lemaître, and G. Faini, J. Phys. Condens. Matter **23**, 446004 (2011).

[22] T. Dietl, H. Ohno, and F. Matsukura, Phys. Rev. B **63**, 195205 (2001).

[23] M. Cubukcu, H. J. von Bardeleben, J. L. Cantin, I. Vickridge, and A. Lemaître, Thin Solid Films **519**, 8212 (2011).

[24] S. Haghgoo, M. Cubukcu, H. J. von Bardeleben, L. Thevenard, A. Lemaître, and C. Gourdon, Phys. Rev. B **82**, 041301(R) (2010).

[25] V. Vlaminck and M. Bailleul, Science **322**, 410 (2008).

[26] M. Zhu, C. L. Dennis, and R. D. McMichael, Phys. Rev. B **81**, 140407(R) (2010).